"Physics of Auroral Phenomena", Proc. XXIX Annual Seminar, Apatity, pp.71-74, 2006

Polar Geophysical Institute

ON THE ELECTRIC POTENTIAL PATTERN CORRESPONDING TO REGION 2 FIELD-ALIGNED CURRENTS DERIVED FROM THE DE2 SATELLITE MEASUREMENTS

I.V.Artamonov[1], E.V.Vasilyeva[1], A.A.Namgaladze[1,2], O.V.Martynenko[1]

[1] *Murmansk State Technical University, Murmansk, Russia*
[2] *Polar Geophysical Institute, Murmansk, Russia*
e-mail: ilyaart@gmail.com

Abstract. The influence of Region 2 field-aligned currents (R2 FAC) on the electric field potential distribution has been studied using the global numerical Upper Atmosphere Model (UAM) for quiet and disturbed conditions. The average R2 FAC distributions obtained by *Maltsev and Ostapenko* [2003] from the Dynamics Explorer 2 satellite data have been used as the model input. As a result of our simulation, we have obtained that the DE2 data provide the almost classical two-vortex electric potential pattern with visible shielding effect for the quiet conditions, but there is the severe electric potential corruption with the over-shielding for the disturbed conditions.

1. Introduction

Field-aligned currents (FAC) were identified for the first time by *Zmuda and Armstrong* [1974] using the magnetometer data from the TRIAD satellite and more systematically studied by *Iijima and Potemra* [1976a, 1976b, 1978] (Fig.1).

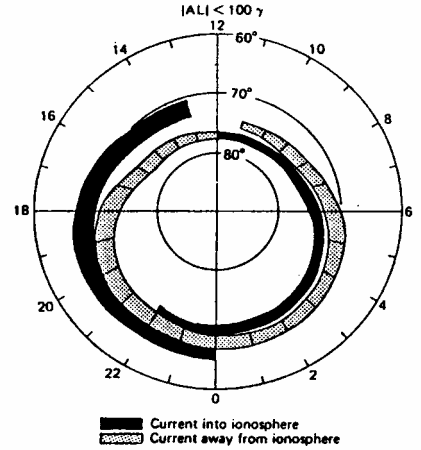

Fig. 1. Average distribution of Region 1/Region 2 field-aligned currents observed by TRIAD.

The magnetosphere-ionosphere electric current system consists of two principal parts: 1) Region 1 field-aligned currents (R1 FAC) connected with the main electric field, 2) Region 2 field-aligned currents (R2 FAC) closed to the partial ring current arising due to the polarization of the drifting plasma. The R1 FAC flows into the ionosphere at the dawnside and flows out at the duskside while the R2 FAC has the opposite direction. The R1 FAC and R2 FAC were predicted in the works by [*Schield et al.*, 1969; *Jaggi and Wolf*, 1973; *Lyatsky et al.*, 1974] and experimentally obtained by *Iijima and Potemra* [1976a]. The location and magnitude of these currents were studied by *Iijima et al.* [1984]; *Potemra et al.* [1984]; *Erlandson et al.* [1988], *Maltsev and Ostapenko* [2003]. *Watanabe et al.* [1998] investigated FAC in the magnetospheric steady state, while *Hoffman et al.* [1994] and *Weimer* [1999] have investigated FAC during substorms. The FAC seasonal dependence was examined by *Fujii et al.* [1981] and *Christiansen et al.* [2002].

Despite several decades of research, there are still many controversies on FAC features and characteristics.

We studied the response of the electric potential distribution to the R2 FAC variations using the global numerical Upper Atmosphere Model (UAM) [*Namgaladze et al.*, 2006], which solves a system of the time-dependent 3D continuity, momentum and heat balance equations for the neutral, ion and electron gases and the electric potential equation.

2. DE2 data description

For the model calculations, we used processed average FAC distributions derived from the magnetic field measurements of DE2 satellite by *Maltsev and Ostapenko* [2003]. They grouped experimental data in 2 sets: for quiet (left plot in Fig. 2) and disturbed (right plot in Fig. 2) conditions.

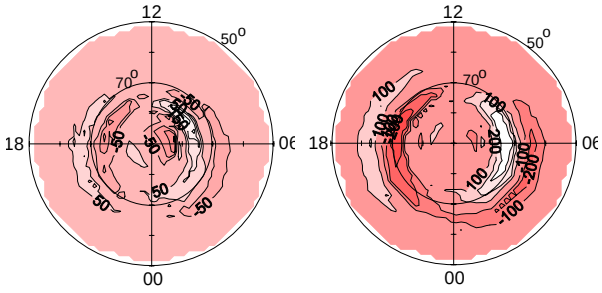

⟨*AL*⟩ = -42 ⟨*AL*⟩ = -313

Fig. 2. Spatial distribution of field-aligned currents in mA/km^2 for |*AL*| < 100 (left plot) and |*AL*| > 100 (right plot). The downward currents are shown by white; the upward currents are shadowed [as given in *Maltsev and Ostapenko*, 2003]

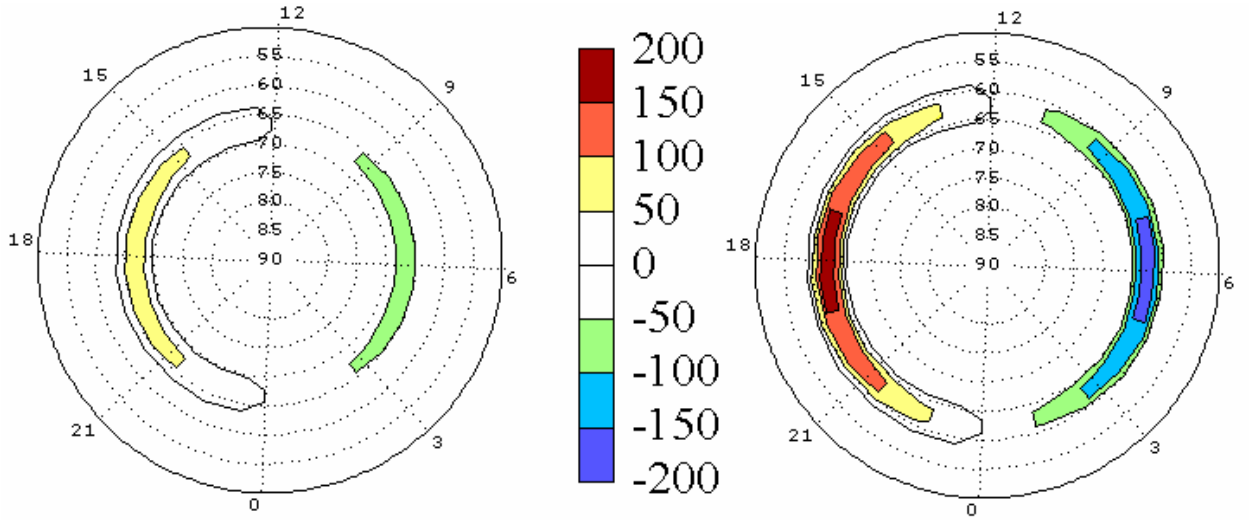

Fig. 3. Geomagnetic polar plots (latitudes 50°-90°N) of downward region 2 field-aligned currents distributions (in mA/km^2) used as the model input in UAM calculations for quiet (left) and disturbed (right) conditions. The Sun position is at the top.

The main features of the quiet (AL-index about -42) FAC include: the R1 FAC are located at 75° geomagnetic latitude, whereas R2 FAC are located at 65° geomagnetic latitude. The average maximum R2 FAC magnitude is approximately 80 mA/km^2.

The right plot in Figure 2 represents the disturbed conditions (AL-index about -313), for which the auroral oval is widened and the FAC system is displaced equatorward to 71° geomagnetic latitude for R1 FAC and to 61° geomagnetic latitude for R2 FAC. The average maximum R2 FAC magnitude is approximately 160 mA/km^2.

3. Simulation technique

Figure 3 shows our model approximation of Maltsev and Ostapenko R2 FAC distribution, which was used as input for the electric potential calculation. The left panel is for the quiet conditions and the right panel is for the disturbed conditions. The presented distribution maps are in the polar coordinates in latitude versus magnetic local time; the noon is at the top and the North Pole is in the center. The next figures of the potential distributions are presented in the same form.

According to the paper by *Maltsev and Feshchenko* [2003] about polar cap voltage relationship to geomagnetic indices, we used two analytical dependencies to find approximate values of Kp-index and the Cross Polar Cap Potential Drop (CPCPD) which is one of the main UAM driving:

$$CPCPD = 0.089\,AE + 38$$
$$CPCPD = 13.3\,Kp + 26.4$$

Using these approximations, we estimated the Kp-index of 1.5 for the quiet and Kp-index of 5 for the disturbed conditions, thus the CPCPD estimations to be used as the model input were 40 kV and 95 kV, respectively.

We performed two variants of simulation. In the first variant the R1 FAC distribution was calculated in the UAM model so as to provide the estimated potential drop. Then, using the ionospheric conductivities, calculated in the other part of the UAM model, the global electric potential distribution was calculated.

In the second variant, additionally the processed satellite experimental data was used for setting R2 FAC distribution. After that we calculated total global electric potential distribution taking into account both R1 and R2 FAC.

Thus we got two electric potential distributions for each of geophysical conditions – one with the R1 FAC only and one with the full FAC system. If we compare these distributions we can identify the effect of the R2 FAC – the shielding of medium and lower latitudes from high-latitudinal electric field.

4. Simulation results

Figure 4 presents the calculated electric potential distributions for quiet (left panel) and disturbed (right panel) conditions. The calculated electric potential distribution for the R1 FAC only (top panel) are labeled as *a* and *c*, and for the both R1 and R2 FAC (middle panel) are labeled as *b* and *d*.

The complete current system provides almost classical two-vortex structure of the electric potential distribution for the quiet conditions.

From the comparison of these polar plots, one can see the visible decrease of the electric field in the middle latitudes known as shielding effect. More clearly it can be seen on the latitude profile along the evening 20MLT-meridian (bottom panel in the Fig. 4).

In the disturbed situation the classic potential pattern became corrupt. Two large ‘petals’ of the opposite sign appeared around midnight at the evening-night and morning-night sides. The analysis of the latitude profile along the evening 20MLT-meridian shows that the shielding electric field became almost as large the dawn-to-dusk electric field.

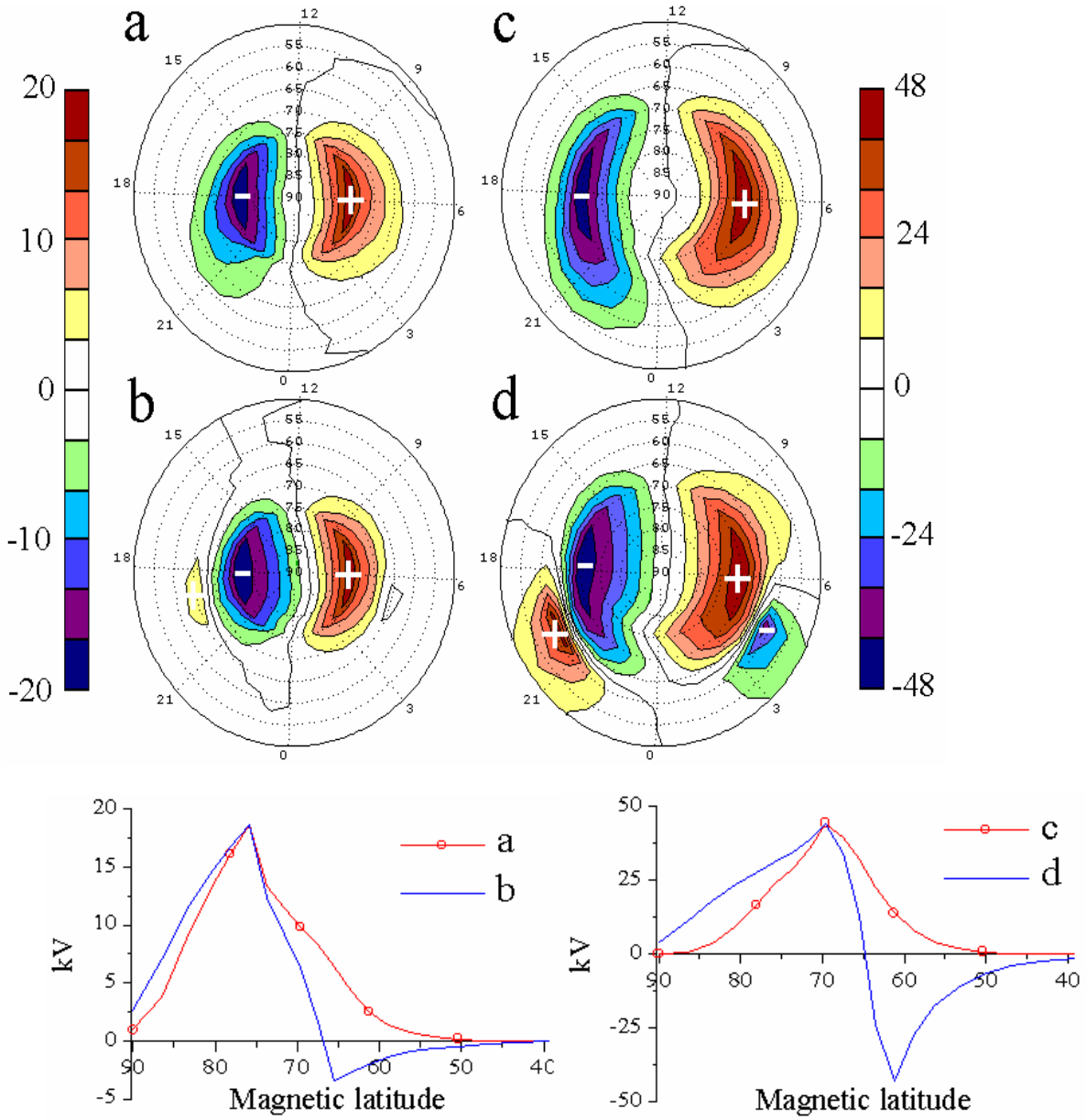

Fig. 4. Geomagnetic polar plots (latitudes 50°-90° N) of the electric potential distribution (in kV) for quiet (left column) and disturbed (right column) conditions: (a) and (c) are with R1 FAC only; (b) and (d) are with both R1 and R2 FAC. The Sun position is at the top. In the bottom there are latitudinal profiles of electric potential along the evening 20MLT-meridian.

5. Discussion

The primary electric field, corresponding to R1 FAC, generates R2 FAC and corresponding secondary electric field. The increase of R2 FAC results in the increase of the secondary field and this field becomes comparable and even larger than the primary field ("over-shielding").

As a result, the night zonal plasma flow becomes converging near midnight instead of diverging in agreement with the observations. Such behavior was observed, for example, by the Millstone Hill incoherent scatter radar during the 15-16 April 2002 events [*Goncharenko*, 2005].

Maltsev and Ostapenko also presented the Total Current Intensity dependence on Kp index, and it approximately was equal to 0.56 for Kp=1.5 and 1.2 MA for Kp=5, while our values were 0.37 and 0.94, respectively.

The problem that we faced is that if we increase the Total Current Intensity to those of Maltsev's, then consequently we have to increase the FAC magnitude or breadth, or both. And then we have very strong over-shielding and the electric potential pattern is very different from average observations. Nevertheless, the presented R2 FAC density distributions do not differ

significantly from those in Maltsev and Ostapenko article.

Acknowledgments. This study was supported by the Russian Basic Research Foundation (grant N05-05-97511). We are grateful to Dr. M. Volkov for the valuable comments and critics.

References

Christiansen, F., V. O. Papitashvili, and T. Neubert (2002), Seasonal variations of high-latitude field-aligned currents inferred from Ørsted and Magsat observations, *J. Geophys. Res.*, *107*(A2), 1029, doi:10.1029/2001JA900104.

Erlandson, R. E., L. J. Zanetti, T. A. Potemra, P. F. Bythrow, and R. Lundin (1988), IMF B_y dependence of region 1 Birkeland currents near noon, *J. Geophys. Res.*, *93*(A9), 9804–9814.

Feshchenko E. Yu., Yu. P. Maltsev (2003), Relation of the polar cap voltage to the geophysical activity, Proc. of 26th Annual Seminar "Physics of Auroral Phenomena", Apatity, 59-61.

Fujii, R., T. Iijima, T. A. Potemra, and M. Sugiura (1981), Seasonal dependence of large-scale Birkeland currents, *Geophys. Res. Lett.*, *8*(10), 1103–1106.

Goncharenko, L., J. E. Salah, A. Van Eyken, V. Howells, J. P. Thayer, V. I. Taran, B. Shpynev, Q. Zhou, J. Chau (2005), Observations of the April 2002 geomagnetic storm by the global network of incoherent scatter radars, *Ann. Geophys.*, *23*(1), 163-181.

Hoffman, R. A., R. Fujii, and M. Sugiura (1994), Characteristics of the field-aligned current system in the nighttime sector during auroral substorms, *J. Geophys. Res.*, *99*(A11), 21,303–21,326.

Iijima, T., and T. A. Potemra (1976a), The amplitude distribution of field-aligned currents at northern high latitudes observed by TRIAD, *J. Geophys. Res.*, *81*(A13), 2165–2174.

Iijima, T., and T. A. Potemra (1976b), Field-aligned currents in the dayside cusp observed by TRIAD, *J. Geophys. Res.*, *81*(A34), 5971– 5979.

Iijima, T., and T. A. Potemra (1978), Large-scale characteristics of field-aligned currents associated with substorms, *J. Geophys. Res.*, *83*(A2), 599–615.

Iijima, T., T. A. Potemra, L. J. Zanetti, and P. F. Bythrow (1984), Large-scale Birkeland currents in the dayside polar region during strongly northward IMF: A new Birkeland current system, *J. Geophys. Res.*, *89*(A9), 7441–7452.

Jaggi, R. V., and R. A. Wolf (1973), Self-consistent calculation of the motion of a sheet of ions in the magnetosphere, *J. Geophys. Res*., *78*(16), 2852-2866.

Lyatsky, W. B., Y. P. Maltsev, and S. V. Leontyev (1974), Three-dimensional current system in the different phases of a substorm, *Planet. Space Sci.*, *22*(8), 1231-1247.

Maltsev, Yu. P., and A. A. Ostapenko (2003), Field-aligned currents in the ionosphere and magnetosphere, Proc. of the Int. Symposium "Auroral Phenomena and Solar-Terrestrial Relations", February 4-7, 2003, Space Research Institute, Moscow, Russia.

Namgaladze A. A., Yu. V. Zubova, A. N. Namgaladze, O. V. Martynenko, E. N. Doronina, L. P. Goncharenko, A. Van Eyken, V. Howells, J. P. Thayer, V. I. Taran, B. Shpynev, and Q. Zhou (2006), Modelling of the ionosphere/thermosphere behaviour during the April 2002 magnetic storms: A comparison of the UAM results with the ISR and NRLMSISE-00 data, *Adv. Space Res.*, *37*(2), 380-391, doi:10.1016/j.asr.2005.04.013.

Potemra, T. A., L. J. Zanetti, P. F. Bythrow, A. T. Y. Lui, and T. Iijima (1984), B_y-dependent convection patterns during Northward interplanetary magnetic field, *J. Geophys. Res.*, *89*(A11), 9753–9760.

Schield, M. A., J. W. Freeman, and A. J. Dessler (1969), A source for field-aligned currents at auroral latitudes, *J. Geophys. Res.*, *74*(1), 247-256.

Watanabe, M., T. Iijima, M. Nakagawa, T. A. Potemra, L. J. Zanetti, S. Ohtani, and P. T. Newell (1998), Field-aligned current systems in the magnetospheric ground state, *J. Geophys. Res.*, *103*(A4), 6853–6870.

Weimer, D. R. (1999), Substorm influence on the ionospheric electric potentials and currents, *J. Geophys. Res.*, *104*(A1), 185–198.

Zmuda, A. J., and J. C. Armstrong (1974), The diurnal flow pattern of fieldaligned currents, *J. Geophys. Res.*, *79*, 4611 –4619.